Trans. Phenom. Nano Micro Scales, 8(2): 117-125, Summer and Autumn 2020
DOI: 10.22111/tpnms.2020.32717.1183

ORIGINAL RESEARCH PAPER

Enhancement of CO_2 mass transfer using SiO_2 nanoparticles in an aqueous a-MDEA solution for CO_2 absorption process

Hossein Shahraki , Jafar Sadeghi , Farhad Shahraki, Davod Mohebbi-Kalhori*

Chemical Engineering Department, University of Sistan and Baluchestan, Zahedan, Iran

Received 17 December 2019; revised 24 July 2020; accepted 6 August 2020; available online 10 November 2020

ABSTRACT: This study investigates the effect of adding SiO_2 nanoparticles to the amine solution on the mass transfer coefficients with the aim to obtain effective solvent in the CO_2 capturing process. An aqueous mixture of the methyl di-ethanol amine (MDEA), activated by blending with Piperazine (PZ) (a-MDEA), was considered as base absorption solvent. The addition of SiO_2 nanoparticles with six different concentrations to the base absorption solvent was then studied. The absorption process took place in an agitated batch reactor at 40 ºC. Considering the gas pressure drop in the reactor the CO_2 absorption and mass transfer rates were obtained for all types of the solvents and were compared with each other. Results revealed that two regimes of fast and slow were involved in the CO_2 absorption process, where the overall mass transfer of the fast regime was more than 100 times that of the slow one. The results indicated that the liquid phase controlled the mass transfer in the CO_2 absorption process. Furthermore, the maximum increase in the absorption rate was happenned when the concentration of SiO_2 nanoparticles was set at 25 ppm in the solvent. In this regard, the enhancement was at least 85% increase in the overall mass transfer coefficient. The findings of this study can be used to design new nanoparticle-based solvents and reduce the cost of the CO_2 capturing process.

KEYWORDS: *CO_2 absorption; CO_2 gas mass transfer; Nano-solvent; Piperazine; SiO_2 nanoparticles.*

INTRODUCTION

Among all the factors responsible for global warming, the carbon dioxide in the atmosphere is the most significant one. Therefore, nowadays, many studies and projects are directed to find or design more effective absorption solvents [1-7] with the aim of reducing energy and cost in the CO_2 absorption process. Aqueous solutions of various amines are used mostly for CO_2 absorption from flue gases and other chemical and petrochemical processes [8]. Monoethanolamine (MEA), Di-ethanol amine (DEA) and Methyl di-ethanol amine (MDEA) are usual in related industries [9]. MEA and DEA have more rapid reaction rates with CO_2 compared to MDEA, but their required regeneration energy is higher than that of MDEA. In this regard, nowadays, using MDEA an activator that improves the reaction rate and therefore the performance of the process is a desire [10]. The MDEA solution activated with a small amount of Piperazine (PZ), called as a-MDEA, is one of the most utilized solvents for the CO_2 capturing process. Numerous studies have been directed on the influence of PZ on the CO_2 absorption when it is mixed up with other alkanol amines. The results depicted an upper reaction rate with CO_2 for the a-MDEA than MDEA [11]. In fact, some benefits of the a-MDEA, compared to MDEA, are more absorption capacity, greater CO_2 reaction rate, and low energy consum-ption for solvent regeneration [12-13].

The CO_2 absorption with an amine solution is a chemical absorption process. The most resistance for this absorption was associated with the diffusion of CO_2 from the gas phase to the liquid phase. The mass transfer resistance on the interfacial surface of the two phases is the important element of decreasing the absorption rate [14]. Some investigations reported increasing the mass transfer rate by adding nanoparticles to the solvent [6-7,15]. For instance, the influence of adding magnetic SiO_2, Fe_3O_4, and Al_2O_3, nanoparticles in the mass transfer rate from the gas phase to liquid phase was studied [16] and was reported significant improvement in the mass transfer rate. Park and Choi studied the effect of silica nanoparticles with a particle size of 12nm on the CO_2 absorption rate using DEA aqueous base solution [17]. They observed a significant reduction in absorption rate and mass transfer coefficient [18]. Also, Hwang and Park examined the influence of SiO_2 nanoparticles and detected an increase in the CO_2 absorption rate [19]. In addition, Kim et al. considered the CO_2 absorption by water mixed with nanoparticles [20]. They found that the absorption increased by 24%. Komati and Suresh reported the influence of magnetic Fe_3O_4 nanoparticles on the mass transfer coefficient that increased by 8.92% [21]. In the other works, the effect of TiO_2 nanoparticles on the mass transfer rate on the enhancement of CO_2 absorption was studied.

✉ *Corresponding Author Email: *davoodmk@@eng.usb.ac.ir*
Tel.: +985431136469; Note. This manuscript was submitted on December 17, 2019; approved on August 6, 2020; published online November 10, 2020.

Nomenclature

A	Area of mass transfer (cm^2)	P_{CO_2}	CO_2 partial pressure in bulk of gas phase (atm)
C_{AL}	Concentration of CO_2 in bulk of liquid phase ($^{mol}/_{cm^3}$)	$P^*_{CO_2}$	CO_2 partial pressure in interface of two phases (atm)
dn_{CO_2}	Number of CO_2 moles that transfer form gas phase to liquid phase in time interval (mol)	$P^0_{CO_2}$	CO_2 partial pressure in start time of interval (atm)
dP_{CO_2}	CO_2 partial pressure decrease (atm)	$P^t_{CO_2}$	CO_2 partial pressure at spent t time (atm)
dt	Time interval (s)	R	Universal gas constant ($^{atm.\,cm^3}/_{K.\,mol}$)
E	Enhancement of CO_2 absorption with reaction relative to without reaction (-)	T	Temperature (K)
H	Henry's constant ($^{atm.\,cm^3}/_{mol}$)	V_g	Gas phase volume of reactor (cm^3)
K_G	Overall mass transfer coefficient in gas phase($^{mol}/_{atm.\,s.\,cm^2}$)	V_l	Liquid phase volume of reactor (cm^3)
k_G	Gas phase mass transfer coefficient ($^{mol}/_{atm.\,s.\,cm^2}$)	Z	Gas compressibility factor (-)
k_L	Liquid phase mass transfer coefficient ($^{mol}/_{atm.\,s.\,cm^2}$)	t	Time (s)
N_{CO_2}	Number of CO_2 moles in unit of time and area that transferred between phases ($^{mol}/_{s.\,cm^2}$)		

In this regard, Li et al. reported the effect of adding TiO_2 nanoparticles and increment in absorption by 11.5% [22]. Also, Zhang et al. (2016) investigated the enhancement of CO_2 absorption by propylene carbonate in the presence of TiO_2 nanoparticles, showing significant improvement. The influences of solids loading and particle size of TiO_2 nanoparticles on the absorption rate were studied experimentally [23]. Their results showed that the gas absorption rate could be enhanced significantly in the presence of TiO_2 nanoparticles and the CO_2 absorption enhancement factor firstly increases and then decreases with the increases of solids loadings [23]. Also Karamian et al. reported up to 71% improvement in mass transfer coefficient for CO_2 absorption by nanofluids such as water/Al_2O_3, water/Fe_2O_3, water/SiO_2 [24]. As well as have been studied effect nanoparticles size (10 up to 60 nm) on CO_2 absorption by water/SiO_2 and was shown increasing mass transfer by increasing nanoparticle size [25].

As mentioned above, there are some results in the literature about the enhancement of the CO_2 absorption rate in the presence of nanoparticle additive in solvents. The reported results indicate quantitatively different values due to that some research was attended to reaction whiles the others were not. It should be noted that the CO_2 absorption with a liquid solvent in the presence of chemical reaction has two steps in series include mass transfer and reaction. The mass transfer or chemical reaction rate is the limiting step depends on the solvent types and mass transfer conditions [11, 26]. As a-MDEA has higher thermodynamic efficiency [27] and is a most widely used solvent in industrial applications, it would need to study the effect nanoparticles in a-MDEA solution on the enhancement of mass transfer rate between gas and liquid phases in the CO_2 absorption process. The purpose of this research is to study the influence of SiO_2 nanoparticles on mass transfer phenomena in the liquid phase for the carbon dioxide absorption process using an aqueous solution MDEA and PZ in order to improve the adsorption process performance. The experiments have been carried out in a standard agitated reactor using several concentrations of the SiO_2 nanoparticles additive in the aqueous amine solvent. The effect of nanoparticles added to the absorption solvent was studied with measuring the CO_2 absorption rate. Consequently, the performance improvement and on the overall mass transfer coefficient were compared with the conventional a-MDEA solvent. Thereupon the investigation was conveyed to find an optimal concentration of nanoparticle additive with a maximum mass transfer rate for CO_2 absorption.

MATERIALS AND METHODS

Chemical Components

Chemical materials and SiO_2 nanoparticles used in this research are the same as our previous report [28]. In brief, the absorption solvent makes with 28%wt. MDEA, 2.5%wt. PZ and 69.5%wt. Distilled water while SiO_2 nanoparticles were added to the absorption solvent in various concentrations. The nanoparticles were mixed with liquid phase using a liquid high shear mixer besides the ultrasonic probe [7]. The mixing procedure was carried out as described by [28]. Six samples with 0, 12.5, 25, 50, 75, 100 ppm concentration of the nanoparticles were prepared with the above procedure. Also, the samples were served to the absorption and desorption process periodically at 40 and 120ºC and after that, all samples tested for the stability of the nanoparticles for 24 hours.

Apparatus

The experimental setup in this research is the same as stated in [28] and depicted in Figure 1. The reactor was equipped with a jacket and an agitator. The reactor volume was 994 mL with a 90 mm ID and a 160 mm height. The agitator has two impellers for both gas and liquid phases. The speed of the mixer is 1000 RPM, which it causes a good liquid mixing. The reactor's wall had not baffle. Therefore,

the liquid phase rotates like a rigid phase and forms a parabolic shape. Thus at interfacial could exist thin layer. The feed gas was entered from the top of the reactor. A water circulator with an external temperature controller used for the reactor's temperature control.

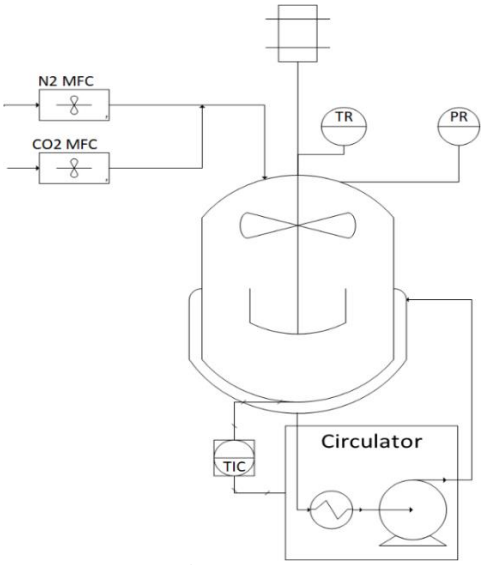

Fig. 1. Laboratory Apparatus for absorption tests comprise the reactor and the instruments system includes some digital measuring devices for the pressure, temperature in gas and liquid phase and mass flow (adapted from (28)).

Furthermore, the apparatus was furnished with a data acquisition system. The reactor's temperature (in gas and liquid phases), pressure, and volume of CO_2 and N_2 gases were recorded by the data acquisition system as well. All data acquired at a data sampling frequency of 1 second. The trends of the reactor's temperatures and pressure versus time were monitored. The precision of the pressure and temperature instruments were ±0.0175 bar and ±0.25ºC, respectively [28].

Mass transfer measurement procedure

In the beginning, the reactor was vacuumed until 40 mbar for air venting and then 500 g of the absorption solvent was supplied to the reactor. Then the reactor's mixer and the water circulator were instantly switched on to control the reactor's temperature while rasing up to 40ºC. Meanwhile, N_2 was injected to pressurize the reactor up to 10 bar. As the reactor's temperature became changeless about 40ºC, the reactor's mixer was cut off and 8000 ml of normal standard CO_2 was injected into the reactor. Following, the CO_2 injection was stopped and the mixer turned on again. The pressure then started to reduce due to fast rate of reaction of CO_2 and its absorption with the amine. The interface depth between gas and liquid was very narrow when the reactor's mixer was off and, consequently, the mass transfer was very low as compared to the reactor's mixer was on. As soon as the absorption completed, the pressure became stable at an equilibrium value. At this time, the reactor's mixer was turned off and feeding of CO_2 gas was started again very fast into the reactor until the reactor's pressure went up to 18 bar. Then, the feeding was stopped and simultaneously the mixer was started. At the second stage of the absorption process and as the result of fast rate of the CO_2 mass transfer and absorption, the reactor's pressure went to decrease rapidly. After spending enough time, when the reactor's pressure became stable and an hour after the reactor's pressure being constant, the mixer was stopped. This procedure included a two-step of CO_2 injection; the amine solution was initially free of CO_2 and therefore the mass transfer and reaction were very rapid. In the second step of CO_2 loading, as the absorption solution had firstly been loaded by CO_2, the pressure drop decrease due to mass transfer were occurred slower. The latter rate of mass transfer were happened due to the small concentration gradient of the CO_2 between liquid and gas phases. During the absorption test, the pressure and temperature of the reactor were recorded every 1 second and the mass transfer rate was obtained using the recorded data.

Mass transfer coefficient calculation method

The mass transfer can be calculated based on the overall gas-phase mass transfer coefficient at any time by equation 1.

$$N_{CO_2} = K_G\left(P_{CO_2} - P^*_{CO_2}\right) \quad (1)$$

where K_G is the overall mass transfer coefficient and defines by equation 2.

$$\frac{1}{K_G} = \frac{1}{k_G} + \frac{H}{Ek_L} \quad (2)$$

The equilibrium between gas and liquid phases for CO_2 defines by Henry's law obtained by equation 3:

$$P^*_{CO_2} = HC_{AL} \quad (3)$$

N_{CO_2} is the rate of CO_2 moles transferred from the gas to liquid phase per unit of surface area. $P^*_{CO_2}$ is the CO_2 partial pressure at the interface of the gas and liquid phases, which is in equilibrium with the CO_2 concentration in the liquid phase ($C_{A,\,L}$). $P_{\,CO_2}$ is the CO_2 partial pressure in the gas phase of the reactor. H is Henry's constant and E is the coefficient of enhanced absorption in the presence of the chemical reaction.

In a better word, E is the fraction of absorption flux with and without reaction. The CO_2 moles that transferred from the gas to liquid phase have been calculated using the pressure drop of the reactor and real gas law. The pressure and temperature have been recorded for each experiment, however, the temperature kept constant during the experiments. At the beginning of the test, the partial pressure of CO_2 is $P^0_{CO_2}$. After t seconds, it decreased to $P^t_{CO_2}$ due to the CO_2 mass transfer to the liquid phase. The CO_2

concentration in the liquid phase was calculated by equation 4.

$$C_{Al} = \frac{dn_{CO_2}}{V_l} = \frac{(P^0_{CO_2} - P^t_{CO_2})V_g}{ZRTV_l} \quad (4)$$

where dn_{CO_2} is the moles of CO_2 that transferred to the liquid phase and V_l is the volume of the amine mixture [23, 29-32]. In the test procedure, firstly, the pressure was stabilized by N_2 gas injection and the CO_2 gas was fed to the reactor. Therefore, the partial pressure of CO_2 calculated using known N_2, T, P, V_g. In addition, at the equilibrium condition, $C_{A,l}$ can be calculated while Henry's constant for each solvent is known as equation 3. The equations for mass transfer from the pressure drop that happens during the absorption phenomenon can be obtained by equation 5.

$$N_{CO_2} = \frac{1}{A}\frac{dn_{CO_2}}{dt} = \frac{-V_g}{ZART}\frac{dP_{CO_2}}{dt} \quad (5)$$

dP_{CO_2}: the reactor's pressure change
V_g: volume of the gas phase in the reactor
T: the reactor's temperature that was constant at 40°C
R: gas constant 83.14 bar.cm^3/Kg-mole
Z: is the gas compressibility factor and for gas mixture in the experiments is 0.965
A: is the mass transfer surface area at the interface

From equations 1, [3-4] and 5 it can be produced a new equation for calculating the overall mass transfer coefficient such as equation 6.

$$-\frac{V_g}{ZART}\frac{dP_{CO_2}}{dt} = K_G\left(P_{CO_2} - \left(\frac{HV_g}{ZRTV_l}\right)\left(P^0_{CO_2} - P_{CO_2}\right)\right) \quad (6)$$

$$h = \left(\frac{HV_g}{RTV_l}\right) \quad (7)$$

with using h expression and rearranging the equation 6, one will obtain the differential equation equation 8.

$$\frac{dP_{CO_2}}{ZP_{CO_2} - hP^0_{CO_2} + hP_{CO_2}} = -(K_G A)\left(\frac{RT}{V_g}\right)dt \quad (8)$$

Integrating of equation 8 from the absorption starting time until ending time (as equation 9) results in an expression for calculation of the overall mass transfer coefficient (equation 10).

$$\int_{P^0_{CO_2}}^{P^t_{CO_2}} \frac{dP_{CO_2}}{(Z+h)P_{CO_2} - hP^0_{CO_2}} = \int_0^t (-K_G A)\left(\frac{RT}{V_g}\right)dt \quad (9)$$

$$K_G \times A = \frac{V_g V_l}{(ZRTV_l + HV_g)t} \ln \frac{ZP^0_{CO_2}}{(Z+h)P^t_{CO_2} - hP^0_{CO_2}} \quad (10)$$

The mass transfer coefficient can be calculated using equation 10. $P^0_{CO_2}$ and $P^t_{CO_2}$ are the partial pressure of CO_2 in the reactor at absorption starting and ending points, respectively. K_G can be calculated at any time interval by using the pressure of the reactor at the starting and ending of the absorption process. A is the mass transfer surface area of the parabolic interface.

RESULTS

In order to get better reliability, every experiment was done at least two times with repeatability and mean values were used for calculation. The experiments for CO_2 mass transfer measuring were done for six solvents having different SiO_2 nanoparticle concentrations that were prepared with the abovementioned procedure. The recorded reactor's pressure versus time and the resulting curve for all solvents is shown in Figure 2.

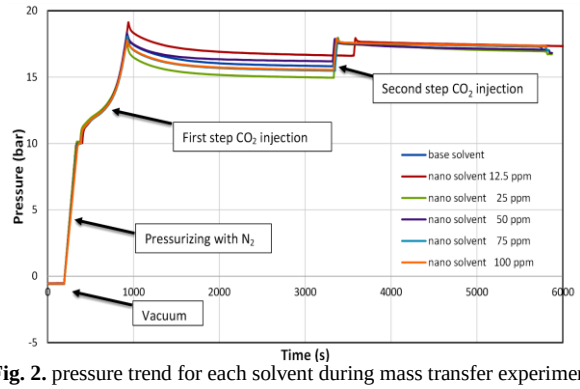

Fig. 2. pressure trend for each solvent during mass transfer experiment include vacuum, N2 pressurizing and two-step CO_2 injection

The experiments were done under similar conditions for all six solvents. Figure 2 depicts two steps of the CO_2 injection.

The portion of curves that is related to the absorption process in the first step of CO_2 injection was zoomed out in Figure 3.

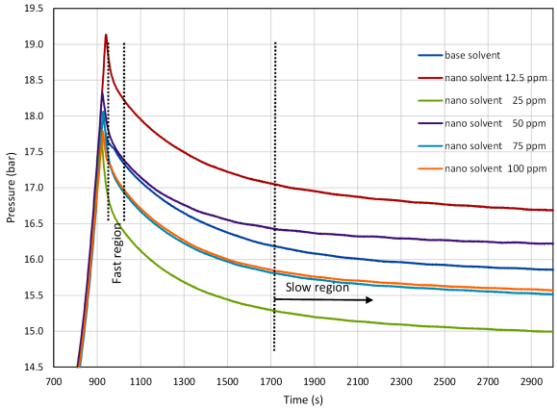

Fig. 3. Pressure trend for each solvent in the absorption experiment during the first step CO_2 injection

It indicates that during the absorption process there are two different pressure drop rate regions or consequently two different mass transfer rate regimes. In the first region, there are a very rapid pressure drop causes of a fast mass transfer from the gas to liquid phase due to a very rapid reaction in the liquid phase. After 60-80 seconds the liquid phase would be rich of CO_2, therefore the concentration of spices would attain an equilibrium value and the reaction gets slow. In this situation, it can be seen that the slow pressure drop leads to a slow mass transfer and reaction rate. For each step of the CO_2 injection, it is being seen this behavior of the pressure drop, but the second step of CO_2 injection, it had been dumped because CO_2 and other spices exist in the liquid phase, and therefore, the mass transfer and reaction rate is slower compared to the first step. At the end of the first step when the pressure became constant, and the equilibrium and steady condition in the reactor have been established, the concentration of CO_2 in the liquid phase could be calculated by using equation 4 and Henry's constant for each solvent by equation 3. The calculated Henry's constant was reported in Table 1.

Table 1
Henry's constant calculated for each solvent at 40ºC.

The concentration of SiO_2 nanoparticles in a solvent (ppm)	**H (atm.l/mol)**
0.0	37.24823
12.5	36.0792
25.0	29.02033
50.0	27.89281
75.0	24.34074
100.0	23.30059

Mass transfer in the reactor consists of two regimes: fast and slow, in which these regimes are depicted in Figure 3.

It is known that there is very short contact time in mass transfer equipment; therefore, the mass transfer coefficient at the beginning of the transport process is more important. The mass transfer coefficient can be obtained separately in each regime for each solvent using the pressure drop and real gas law. A time interval in recorded data of the absorption test was selected for each solvent, in which the pressure drop in that interval be linear and smooth. The results of the calculation are presented in Table 2. The curve of $KG \times A$ versus concentration of SiO_2 nanoparticles was shown in Figure 4.

Table 2
Calculated mass transfer coefficient for the fast regime in the first step of the CO_2 injection.

SiO_2 nanoparticles concentration in a solvent (ppm)	**Selected time interval**		**p^0 (atm)**	**P (atm)**	**$KG \times A$ (kmol/(atm.hr)**
	Starting time (s)	**Ending time (s)**			
0.0	931	966	13.20941	12.81612	40.54352
12.5	948	1000	13.8502	13.28268	52.86962
25.0	922	980	12.93757	11.86113	91.17221
50.0	926	964	13.13998	12.53899	78.85339
75.0	933	1020	12.7763	11.81089	57.12795
100.0	930	973	12.4982	12.03228	55.37133

As depicted in Figure 4, Nanofluid with 25 ppm of SiO_2 nanoparticles has the best mass transfer coefficient. In the second step, CO_2 was injected into the reactor following the procedure explained before.

Because in this system, the mass transfer and reaction take place simultaneously, and after the first CO_2 injection, the reactions that take place in the liquid phase become slower, based on equation 2, KG must be lower than the first CO_2 injection.

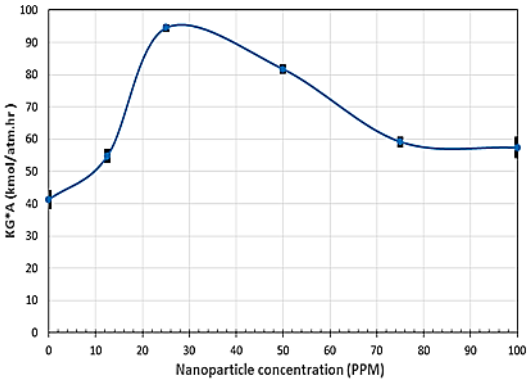

Fig. 4. Calculated $KG \times A$ versus nanoparticle concentration in the first step CO_2 injection for the fast region.

The result for the second CO_2 injection was shown in Figure 5.

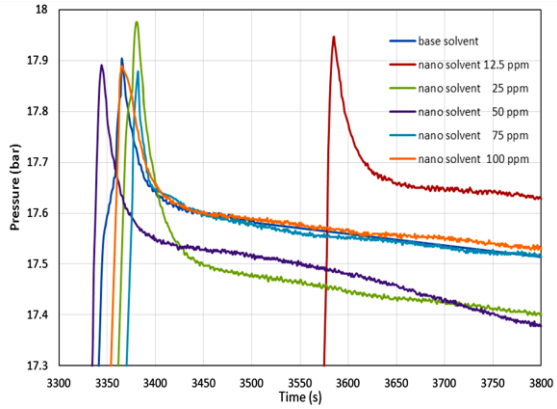

Fig. 5. Pressure trend for each solvent in the absorption experiment during the second step CO_2 injection

For calculation of the mass transfer coefficient for each solvent, a time interval was selected, where the pressure drop curve was linear in that interval and *KG*×*A* could be calculated by equation 10. The results of these calculations were shown in Table 3, and the curve of *KG*×*A* plotted in Figure 6.

Table 3
Calculated mass transfer coefficient for the fast regime in the second step of the CO_2 injection.

SiO_2 nanoparticles concentration in solvent (ppm)	Selected time interval		P^0 (atm)	P (atm)	KG×A (kmol/ (atm.hr)
	Starting time (s)	Ending time (s)			
0.0	3364	3395	11.08429	10.90792	35.06615
12.5	3585	3620	11.52089	11.27414	43.51500
25.0	3381	3421	10.70081	10.27517	65.91678
50.0	3344	3384	10.5943	10.27353	52.42062
75.0	3382	3416	10.22888	9.98744	47.46588
100.0	3365	3403	9.95307	9.71684	42.41464

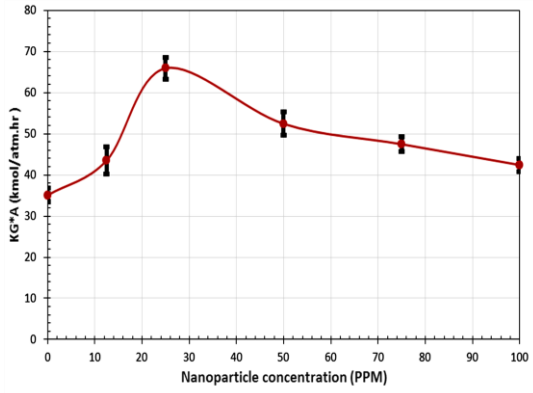

Fig. 6. Calculated *KG**×*A* versus nanoparticle concentration in the second step CO_2 injection for the fast region

KG×*A* was calculated for the slow mass transfer regime from the results shown in Figure 5. The time interval has been selected in the region that pressure decreases slowly and being linear. The *KG*×*A* was calculated using equation10. The results presented in Table 4 and the curve of the mass transfer coefficient was shown in Figure 7.

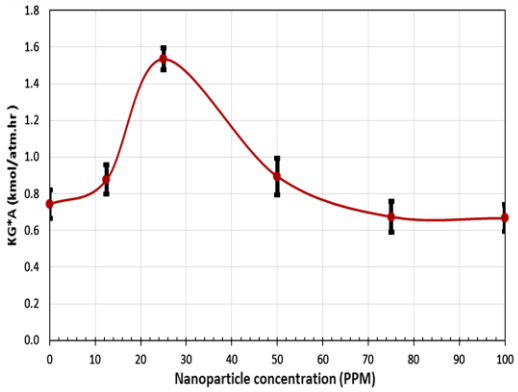

Fig. 7. Calculated *KG*×*A* versus nanoparticle concentration in the second step CO_2 injection for the slow region

Table 4
Calculated mass transfer coefficient for the slow regime in the second step of the CO_2 injection.

Nanoparticles concentration in solvent (ppm)	Selected time interval		P^0 (atm)	P (atm)	KG×A (kmol/ (atm.hr)
	Start time(s)	Ending time(s)			
0.0	3901	5300	10.76913	10.60565	0.74213
12.5	3900	5352	11.19086	10.99037	0.87636
25.0	3723	5631	10.14871	9.70456	1.53381
50.0	4241	5437	9.96509	9.81087	0.89433
75.0	4130	5590	9.82544	9.68356	0.67410
100.0	3950	5650	9.58421	9.42383	0.66664

DISCUSSION

Mass transfer is a phenomenon that arises from the concentration gradient and causes diffuse molecules from a high concentration to low concentration. The film theory is the oldest and the most understood theory for the mass transfer coefficients calculation [34]. In gas absorption, the mass would be transferred from a gas phase to the liquid phase, and if the liquid phase tendency to react with a gas molecule, the absorption rate changes to a faster rate. In this case, the absorption takes place through the physical and chemical absorption steps. In this theory, it was assumed that there is a reaction film on the gas-liquid interface and the mass transfer occurs only through the film (figure 8).

As indicated in Figure 8, there is a very rapid mass transfer regime due to reaction rate and a high CO_2 concentration difference in the liquid phase. This regime would happen at the beginning of the absorption process. After that; the mass transfer would be reduced to a lower rate and would follow a linear dependency between pressure and time or liquid

depth. These two regimes were observed in the experimental results, which is shown in Figures 3 and 5. The equilibrium concentration on the gas-liquid interface has been controlled by the reaction [35-36].

The mass transfer rate was calculated for each time interval using the total pressure drop and real gas law in that time interval. Therefore, for all prepared solvents the mass transfer rate was obtained during the selected time interval. It indicates the amount of mass that has been transferred in the fast regime is more than 100 times relating to the slow regime. In the fast regime, the mass transfer rate is very high because of very fast reaction speed and in the slow regime, the reaction speed is slow because the reactions are in their equilibrium nature. Therefore, the reaction speed will be settled down when the concentration of reactants and products reached the equilibrium value [35, 37].

Two facts were indicated in Figures 4, 6 and 7. Firstly, these figures signify that the controlling phenomenon is the mass transfer in the liquid phase because the absorption rate was influenced in both two steps by the SiO_2 nanoparticles. It is known that when the mass transfer is the controlling mechanism, the nanoparticles can affect the emersions on absorption. Secondly, these figures indicate that in each of the two steps of the CO_2 injection, the maximum mass transfer rate with respect to the base solvent happened at 25 ppm of the nanoparticles concentration.

CONCLUSION

In this research, it has been found that the absorption by the aqueous amine solution has two regimes and SiO_2 nanoparticles influence on both regimes, therefore, the mass transfer in the liquid phase is the controlling phenomenon. Also, it has been found that at 25 ppm of the nanoparticles concentration a maximum mass transfer happened, and so the mass transfer coefficient is a maximum at 25 ppm of the nanoparticles concentration. Experiments indicate improvement in the mass transfer coefficient by increasing nanoparticle concentration to the maximum value. This improvement can be from the Brownian motion of the nanoparticles and induced micro-convection. The mass transfer coefficient decreases at nanoparticles concentration from 25 ppm until to 100 ppm. This is due to reducing in Brownian motion from point of velocity and distance cause of more population of nanoparticles in the liquid phase. At the highest concentration of nanoparticles (100 ppm) mass transfer coefficient is more than the base fluid and this is the response of induce micro-convection. This behavior also reported by J.-Z. Jiang et al. [38] and H.- J. Bart et al. [39].

From $KG \times A$ indicated in Tables 2, 3 and 4, it has been concluded that improvements in the mass transfer coefficient are, 127, 85 and 100 % respect to the base solvent, respectively. Because the mass transfer equipment operates at the fast regime and contact time between phases is about several seconds and solvent have initial CO_2 content. Thereupon 85% improvement is more applicable. Therefore 85% improvement in the mass transfer has been concluded for the whole absorption process. enhancement in the mass transfer coefficient that was reported for CO_2 absorption by other researchers is from 31 up to 90% depending on the material of nanoparticles, size concentration and base solvent [7, 25, 39]. In the previous work, it was shown that the nanoparticles have a positive influence on the CO_2 loading of the solvent [28]. Therefore, it can be concluded that the nanoparticles improved the mass transfer rate of at least 85% at 25 ppm concentration of the SiO_2 nanoparticles. Also, the results indicate that the mass transfer in the liquid phase is the controlling phenomenon in both regimes.

ACKNOWLEDGMENTS

This research was supported by the NPC-RT and the National Petrochemical Company of Iran. The authors are also obliged to managers and employees of the NPC-RT Company for their assistance.

REFERENCES

[1] Li B, Duan Y, Luebke D, Morreale B. Advances in CO_2 capture technology: A patent review. Applied Energy. 2013 Feb 1;102:1439-47.

[2] Zhao B, Tao W, Zhong M, Su Y, Cui G. Process, performance and modeling of CO_2 capture by chemical absorption using high gravity: A review. Renewable and Sustainable Energy Reviews. 2016 Nov 1;65:44-56.

[3] Muhammad A, GadelHak Y. Simulation based improvement techniques for acid gases sweetening by chemical absorption: A review. International Journal of Greenhouse Gas Control. 2015 Jun 1;37:481-91.

[4] Singto S, Supap T, Idem R, Tontiwachwuthikul P, Tantayanon S, Al-Marri MJ, Benamor A. Synthesis of new amines for enhanced carbon dioxide (CO_2) capture performance: The effect of chemical structure on equilibrium solubility, cyclic capacity, kinetics of absorption and regeneration, and heats of absorption and regeneration. Separation and Purification Technology. 2016 Jul 14;167:97-107.

[5] Liang Z, Fu K, Idem R, Tontiwachwuthikul P. Review on current advances, future challenges and consideration issues for post-combustion CO_2 capture using amine-based absorbents. Chinese Journal of Chemical Engineering. 2016 Feb 1;24(2):278-88.

[6] Zhang Z, Cai J, Chen F, Li H, Zhang W, Qi W. Progress in enhancement of CO_2 absorption by nanofluids: A mini review of mechanisms and current status. Renewable energy. 2018 Apr 1;118:527-35.

[7] Yu W, Wang T, Park AH, Fang M. Review of liquid nano-absorbents for enhanced CO_2 capture. Nanoscale. 2019;11(37):17137-56.

[8] Notz R, Asprion N, Clausen I, Hasse H. Selection and pilot plant tests of new absorbents for post-combustion carbon dioxide capture. Chemical Engineering Research and Design. 2007 Jan 1;85(4):510-5.

[9] Khan AA, Halder GN, Saha AK. Comparing CO_2 removal characteristics of aqueous solutions of monoethanolamine, 2-amino-2-methyl-1-propanol, methyldiethanolamine and piperazine through absorption process. International Journal of Greenhouse Gas Control. 2016 Jul 1;50:179-89.

[10] Dubois L, Thomas D. Postcombustion CO_2 capture by chemical absorption: screening of aqueous amine (s)-based solvents. Energy Procedia. 2013 Jan 1;37:1648-57.

[11] Bishnoi S, Rochelle GT. Absorption of carbon dioxide into aqueous piperazine: reaction kinetics, mass transfer and solubility. Chemical engineering science. 2000 Nov 1;55(22):5531-43.

[12] Mudhasakul S, Ku HM, Douglas PL. A simulation model of a CO2 absorption process with methyldiethanolamine solvent and piperazine as an activator. International Journal of Greenhouse Gas Control. 2013 Jul 1;15:134-41.

[13] Xu GW, Zhang CF, Qin SJ, Zhu BC. Desorption of CO_2 from MDEA and activated MDEA solutions. Industrial & engineering chemistry research. 1995 Mar;34(3):874-80.

[14] Puxty G, Maeder M. The fundamentals of post-combustion capture. InAbsorption-based Post-combustion Capture of Carbon Dioxide 2016 Jan 1 (pp. 13-33). Woodhead Publishing.

[15] Beiki H, Esfahany MN, Etesami N. Turbulent mass transfer of Al_2O_3 and TiO_2 electrolyte nanofluids in circular tube. Microfluidics and nanofluidics. 2013 Oct 1;15(4):501-8.

[16] Rahmatmand B, Keshavarz P, Ayatollahi S. Study of absorption enhancement of CO_2 by SiO_2, Al_2O_3, CNT, and Fe_3O_4 nanoparticles in water and amine solutions. Journal of Chemical & Engineering Data. 2016 Apr 14;61(4):1378-87.

[17] Park SW, Choi BS, Lee JW. Chemical Absorption of Carbon Dioxide into Aqueous Colloidal Silica Solution with Diethanolamine. Separation Science and Technology. 2006;41(14):3265-78.

[18] Park SW, Lee JW, Choi BS, Lee JW. Absorption of Carbon Dioxide into Aqueous Colloidal Silica Solution. Separation Science and Technology. 2006;41(8):1661-77.

[19] Hwang BJ, Park SW, Park DW, Oh KJ, Kim SS. Absorption of carbon dioxide into aqueous colloidal silica solution with different sizes of silica particles containing monoethanolamine. Korean Journal of Chemical Engineering. 2009 May 1;26(3):775-82.

[20] Kim WG, Kang HU, Jung KM, Kim SH. Synthesis of silica nanofluid and application to CO_2 absorption. Separation Science and Technology. 2008 Aug 8;43(11-12):3036-55.

[21] Komati S, Suresh AK. CO_2 absorption into amine solutions: a novel strategy for intensification based on the addition of ferrofluids. Journal of Chemical Technology & Biotechnology: International Research in Process, Environmental & Clean Technology. 2008 Aug;83(8):1094-100.

[22] Li SH, Ding Y, Zhang XS. Enhancement on CO_2 bubble absorption in MDEA solution by TiO_2 nanoparticles. InAdvanced Materials Research 2013 (Vol. 631, pp. 127-134). Trans Tech Publications Ltd.

[23] Zhang Y, Zhao B, Jiang J, Zhuo Y, Wang S. The use of TiO_2 nanoparticles to enhance CO_2 absorption. International Journal of Greenhouse Gas Control. 2016 Jul 1;50:49-56.

[24] Karamian S, Mowla D, Esmaeilzadeh F. The effect of various nanofluids on absorption intensification of CO_2/SO_2 in a single-bubble column. Processes. 2019 Jul;7(7):393.

[25] Darvanjooghi MH, Esfahany MN, Esmaeili-Faraj SH. Investigation of the effects of nanoparticle size on CO_2 absorption by silica-water nanofluid. Separation and Purification Technology. 2018 Apr 29;195:208-15.

[26] Idem R, Edali M, Aboudheir A. Kinetics, modeling, and simulation of the experimental kinetics data of carbon dioxide absorption into mixed aqueous solutions of MDEA and PZ using laminar jet apparatus with a numerically solved absorption-rate/kinetic model. Energy Procedia. 2009 Feb 1;1(1):1343-50.

[27] Prentza L, Koronaki IP, Nitsas MT. Investigating the performance and thermodynamic efficiency of CO_2 reactive absorption–A solvent comparison study. Thermal Science and Engineering Progress. 2018 Sep 1;7:33-44.

[28] Shahraki H, Sadeghi J, Shahraki F, Kalhori DM. Investigation on CO_2 solubility in aqueous amine solution of MDEA/PZ with SiO_2 nanoparticles additive as novel solvent. J Chem Eng Process Technol. 2016;7:37-43.

[29] Aouini I, Ledouxa A, Estel L, Mary S, Evrard P, Valognes B. Experimental study of carbon dioxide capture from synthetic industrial incinerator flue gas with a pilot and laboratory measurements. Procedia Engineering. 2012 Jan 1;42:704-20.

[30] Kierzkowska-Pawlak H. Kinetics of CO_2 absorption in aqueous N, N-diethylethanolamine and its blend with N-(2-aminoethyl) ethanolamine using a stirred cell reactor. International Journal of Greenhouse Gas Control. 2015 Jun 1;37:76-84.

[31] Dang H, Rochelle GT. CO_2 absorption rate and solubility in monoethanolamine/piperazine/water. Separation science and technology. 2003 Jan 3;38(2):337-57.

[32] Li L, Rochelle G. CO2 mass transfer and solubility in aqueous primary and secondary amine. Energy Procedia. 2014 Jan 1;63:1487-96.

[33] Perry RH, Green DW, Maloney JOH. Perry's chemical engineers' handbook. 7th ed. United States of America: Mc Grawhill; 1997. 2434 p.

[34] Lewis WK, Whitman WG. Principles of gas absorption. Industrial & Engineering Chemistry. 1924 Dec;16(12):1215-20.

[35] Puxty G, Rowland R. Modeling CO2 mass transfer in amine mixtures: PZ-AMP and PZ-MDEA. Environmental science & technology. 2011 Mar 15;45(6):2398-405.

[36] Norouzbahari S, Shahhosseini S, Ghaemi A. CO2 chemical absorption into aqueous solutions of piperazine: modeling of kinetics and mass transfer rate. Journal of Natural Gas Science and Engineering. 2015 Sep 1;26:1059-67.

[37] Sodiq A, Rayer AV, Abu-Zahra MR. The kinetic effect of adding piperazine activator to aqueous tertiary and sterically-hindered amines using stopped-flow technique. Energy Procedia. 2014 Jan 1;63:1256-67.

[38] Jiang JZ, Zhang S, Liu L, Sun BM. A microscopic experimental study of nanoparticle motion for the enhancement of oxygen absorption in nanofluids. Nanotechnology Reviews. 2018 Dec 19;7(6):529-39.

[39] Sunden B, Salimi Nanagedani F. Prediction of mass transfer coefficient of the continuous phase in a structured packed extraction column in the presence of SiO_2 nanoparticles. Frontiers in Heat and Mass Transfer (FHMT). 2020 Feb 27;14.